

# Statistical analysis of multimode weakly nonlinear Rayleigh-Taylor instability in the presence of surface tension

J. Garnier\*

*Laboratoire de Statistique et Probabilités, Université Paul Sabatier, 118 Route de Narbonne, 31062 Toulouse Cedex 4, France*

C. Cherfils-Clérouin and P.-A. Holstein

*Commissariat à l'Energie Atomique, Direction des Applications Militaires, BP12, 91680 Bruyères le Châtel, France*

(Received 27 February 2003; revised manuscript received 6 June 2003; published 12 September 2003)

A weakly nonlinear model is proposed for the Rayleigh-Taylor instability in the presence of surface tension. The dynamics of a multimode perturbation of the interface between two incompressible, inviscid, irrotational, and immiscible fluids is analyzed. The quadratic and cubic nonlinear effects are taken into account. They include the nonlinear corrections to the exponential growths of the fundamental modulations. The role of the initial modulation spectrum is discussed. A saturation criterion in terms of the product of a local rms and a particular wave number is exhibited. It gives theoretical foundations for numerical conjectures and allows one to analyze the effects of fundamental parameters of the problem such as the dimension or the Atwood number.

DOI: 10.1103/PhysRevE.68.036401

PACS number(s): 52.57.Fg, 52.35.Py, 52.35.Tc

## I. INTRODUCTION

The stability of hydrodynamic flows has been a fundamental issue in fluid mechanics for a long time [1,2]. Recently the Rayleigh-Taylor (RT) instability has attracted a growing attention because of its applications to astrophysics [3] and inertial confinement fusion (ICF) [4]. The RT instability occurs at an interface between a fluid that accelerates another fluid of higher density. This phenomenon may dramatically reduce the performance of ICF experiments by degrading the symmetry of implosion. In classical RT experiments it has been shown that the instability growth is limited by surface tension during the linear stage, where the growth is exponential in time [5]. In ICF experiments the ablation process and the thermal transport are coming into play. The RT growth is stabilized by the flow of material through the ablation front [6]. For both experimental conditions the linear growth rate has a maximum for some wave number.

The aim of this paper is to develop a weakly nonlinear (WNL) theory of the classical RT instability in the presence of surface tension. We have built this theory so as to be able to propose closed-form expressions for the most important physical quantities and to address arbitrary initial perturbations. Recently a multimode WNL theory for the RT instability in the absence of surface tension was presented in the framework of a small finite bandwidth [7,8], but the model can only be integrated numerically. In this paper we are mainly interested in the multimode case, but we first start by stating the results for a single-mode perturbation. We confirm the standard result that the growth of the fundamental mode slows down when its amplitude becomes comparable to its wavelength, and we analytically compute the constant that appears in this relationship.

The evolution of the RT instability from multimode initial

conditions is much more complicated [9–11]. In the linear regime the frequency modes grow independently and exponentially in time with the growth rate that depends on the wave number. The main issue is whether the dynamics is dominated by the mode with the largest initial amplitude or by the mode with the largest linear growth rate. The answer to this question will have dramatic consequences on the WNL regime. Indeed, when the amplitude of the perturbation reaches a critical value, mode coupling becomes possible between a wide range of frequencies and wave numbers. The results of these WNL interactions will strongly depend on the modes that dominate the spectrum of the modulation just before the transition from the linear regime to the WNL regime.

The paper is organized as follows. The description of the interface elevation in terms of a random process is introduced in Sec. II. We present the Hamiltonian formalism of the evolution equations in Sec. III. The single-mode case is briefly discussed in Sec. IV. In Sec. V we study the power spectral density of a multimode interface elevation. The role of the initial spectrum is discussed in Sec. VI.

## II. DESCRIPTION OF THE INTERFACE

We shall study the dynamics of a small-amplitude perturbation of the interface whose displacement with respect to the unperturbed front  $z=0$  is described by  $z = \eta(t, \mathbf{x})$ . The transverse spatial variables  $(x, y)$  are denoted by  $\mathbf{x}$ . It is convenient for the linear and WNL regimes to consider the Fourier modes of the interface

$$\eta(t, \mathbf{x}) = \frac{1}{2\pi} \int d^2\mathbf{k} \exp(i\mathbf{k} \cdot \mathbf{x}) \eta_{\mathbf{k}}(t).$$

Note that in a two-dimensional (2D) configuration,  $x \in \mathbb{R}$ , and we should substitute  $\sqrt{2\pi}$  for  $2\pi$  in the definition of the Fourier transform. In this paper we shall briefly address for consistency the single-mode case

---

\*Electronic address: garnier@cict.fr;  
URL: <http://www.lsp.ups-tlse.fr/Garnier>

$$\eta(0, \mathbf{x}) = \sqrt{2} \sigma_1 \cos(\mathbf{k}_p \cdot \mathbf{x}), \quad (1)$$

which reads in Fourier modes as

$$\eta_{\mathbf{k}}(0) = \sqrt{2} \pi \sigma_1 [\delta(\mathbf{k} - \mathbf{k}_p) + \delta(\mathbf{k} + \mathbf{k}_p)], \quad (2)$$

where the initial amplitude has been normalized so that the rms modulation is  $\sigma_1$ . We shall focus our attention to the multimode case. We shall model the initial perturbation  $\eta(0, \mathbf{x})$  of the interface elevation as the realization of a spatially random process with Gaussian statistics. The statistical distribution of this process is characterized by the two first moments

$$\langle \eta(0, \mathbf{x}) \rangle = 0, \quad \langle \eta(0, \mathbf{x}) \eta(0, \mathbf{x}') \rangle = C(\mathbf{x} - \mathbf{x}'),$$

where the brackets stand for a statistical average and  $C$  is the so-called autocorrelation function. The autocorrelation function of the Fourier transform of  $\eta$  is

$$\langle \eta_{\mathbf{k}}(0) \eta_{\mathbf{k}'}(0) \rangle = \delta(\mathbf{k} + \mathbf{k}') \Gamma_{\mathbf{k}}(0).$$

The positive-valued function  $\mathbf{k} \mapsto \Gamma_{\mathbf{k}}$  is the power spectral density (PSD) defined by

$$\Gamma_{\mathbf{k}}(0) := \int C(\mathbf{x}) \exp(-i\mathbf{k} \cdot \mathbf{x}) d^2 \mathbf{x}.$$

A limit case is the white noise model where the correlation radius of the process is assumed to be very small. The autocorrelation function is then reduced to a Dirac distribution  $C(\mathbf{x}) = \sigma_0^2 \delta(\mathbf{x})$  and the PSD is identically equal to the constant  $\sigma_0^2$ . Please note that  $\sigma_0$  is not a rms, but  $\sigma_0^2$  has the dimension of a length to the power 4 in three dimensions, and to the power 3 in two dimensions.

The choice of a statistical description for the multimode interface is both mathematically and physically relevant. Indeed the initial modulation of the surface is only known approximately. The statistical model takes into account the available data (rms, spectrum) and completes the unknown data by putting a statistical distribution on them. This distribution should be chosen in a natural way, and the most natural model (maximizing the entropy) when only the first two moments are specified is Gaussian statistics. Finally, the choice of Gaussian statistics is also consistent with the empirical picture that the initial interface perturbation originates from many small imperfections: we can then invoke the central limit theorem which claims that Gaussian statistics always results from the contribution of many independent effects [12].

Before introducing the equations governing the dynamics, we would like to comment on the interpretation of the results. We consider a set of possible realizations of the initial perturbation of the interface. From a practical point of view we seek information that holds true for an arbitrary realization of the interface. We are going to compute statistical averages. Throughout the paper we shall focus our attention to the PSD of the modulation. This function actually contains all the information about the spatial process  $\eta$  [12]. The ergodic principle gives the equivalence between the theoret-

ical statistical average and the experimental local or global spatial averages, such as the spatial spectrum or the rms.

### III. THE HAMILTONIAN FORMALISM

We consider an interface  $z = \eta(t, \mathbf{x})$  that separates two incompressible, irrotational, inviscid, and immiscible fluids in a gravitational field  $g$  pointing into the negative  $z$  direction. Evolution equations can be written in Hamiltonian form [13]

$$\frac{\partial \psi}{\partial t} = - \frac{\delta H}{\delta \eta}, \quad \frac{\partial \eta}{\partial t} = \frac{\delta H}{\delta \psi}, \quad (3)$$

with the canonical variables  $\eta$  and the surface potential  $\psi = \rho_1 \phi_1|_{z=\eta} - \rho_2 \phi_2|_{z=\eta}$ . Here  $\phi_1$  ( $\phi_2$ ) is the hydrodynamic potential for the upper fluid (the lower fluid). The Hamiltonian reads as a surface integral

$$H = \frac{1}{2} \int [v_n \psi \sqrt{1 + |\nabla_{\perp} \eta|^2} + (\rho_1 - \rho_2) g \eta^2] d^2 \mathbf{x}.$$

Note that the Hamiltonian seems to depend also on the normal velocity of the interface  $v_n$ . Actually the tricky part of the analysis consists in expressing  $v_n$  in terms of  $\eta$  and  $\psi$ . Such an expression was obtained in the form of a series expansion in Ref. [14]. Surface tension can be included into the model by adding to the Hamiltonian the term

$$H_S = s \int (\sqrt{1 + |\nabla_{\perp} \eta|^2} - 1) d^2 \mathbf{x}.$$

We shall see that the primary effect of surface tension is to stabilize the high-frequency modulations. Indeed classical RT instability exhibits a divergence of the growth rate for growing frequency which involves instantaneous blowup in the white noise case.

The main result derived in Ref. [14] is a systematic way to calculate a closed-form expression of the expansion of the Hamiltonian for arbitrary orders. Explicit formulas for second- and third-order are given in the absence of surface tension. Inclusion of surface tension is a straightforward generalization, and it is found that the Hamiltonian can be expanded in powers of  $\eta$  and  $\psi$  as  $H = \sum_{n=0}^{\infty} H_n$ ,

$$H_n = \frac{1}{2n!(2\pi)^n} \int \cdots \int d^2 \mathbf{k}_0 \cdots d^2 \mathbf{k}_n \eta_{\mathbf{k}_1} \cdots \eta_{\mathbf{k}_n} \\ \times (L_{-\mathbf{k}_1, \mathbf{k}_0, \dots, \mathbf{k}_n} \psi_{\mathbf{k}_1} \psi_{\mathbf{k}_0} + G_{-\mathbf{k}_1, \mathbf{k}_0, \dots, \mathbf{k}_n} \eta_{\mathbf{k}_1} \eta_{\mathbf{k}_0}),$$

where  $\mathbf{k}_i = -\mathbf{k}_0 - \cdots - \mathbf{k}_n$ . Once the expression of the Hamiltonian is known it is theoretically possible to solve the evolution equations (3). Unfortunately the coefficients  $G$  and  $L$  have so complicated expressions that it is impossible to solve analytically the evolution equations and to derive closed-form expressions for  $\eta$ . A tractable approach is a WNL analysis which consists in solving Eqs. (3) recursively. Assuming that the amplitudes of the initial perturbations  $\eta$

and  $\psi$  are small (i.e., smaller than the typical wavelength), we introduce a small dimensionless parameter  $\varepsilon$  so that  $\eta$  and  $\psi$  can be expanded as

$$\eta_{\mathbf{k}} = \sum_{j=0}^{\infty} \varepsilon^{j+1} \eta_{\mathbf{k},j}, \quad \psi_{\mathbf{k}} = \sum_{j=0}^{\infty} \varepsilon^{j+1} \psi_{\mathbf{k},j}.$$

We then substitute these Ansätze into Eqs. (3) and collect the terms with the same powers in  $\varepsilon$ . We obtain by collecting the terms of the order of  $\varepsilon$  the linear system

$$\frac{\partial \eta_{\mathbf{k},0}}{\partial t} = L_{\mathbf{k}}^{(0)} \psi_{\mathbf{k},0}, \quad \frac{\partial \psi_{\mathbf{k},0}}{\partial t} = -G_{\mathbf{k}}^{(0)} \eta_{\mathbf{k},0}. \quad (4)$$

$\psi$  can be eliminated from this system consistent with the appropriate order of perturbation which yields  $\partial_t^2 \eta_{\mathbf{k}} = \gamma_{\mathbf{k}}^2 \eta_{\mathbf{k}}$ , where  $\gamma_{\mathbf{k}}$  is the linear growth rate,

$$\gamma_{\mathbf{k}} = \sqrt{Ag|\mathbf{k}|} \sqrt{1 - \frac{|\mathbf{k}|^2}{3k_{max}^2}}, \quad k_{max} = \sqrt{\frac{(\rho_1 - \rho_2)g}{3s}},$$

$A = (\rho_1 - \rho_2)/(\rho_1 + \rho_2)$  is the Atwood number. Note that the gain curve is maximal for  $|\mathbf{k}| = k_{max}$  and the corresponding maximal gain is  $\gamma_{max} = \sqrt{2Agk_{max}}/3$ . Assuming  $\partial_t \eta_{\mathbf{k}}(0) = 0$ , we get that the Fourier modes in the linear regime grow like hyperbolic cosine:  $\eta_{\mathbf{k}}(t) = \eta_{\mathbf{k}}(0) \cosh(\gamma_{\mathbf{k}} t)$ . If  $\eta_{\mathbf{k}}(0)$  corresponds to a white noise, then  $\eta$  has Gaussian statistics and its PSD is

$$\Gamma_{\mathbf{k}}(t) = \sigma_0^2 \cosh^2(\gamma_{\mathbf{k}} t). \quad (5)$$

After a short transition time, as soon as  $\gamma_{max} t > 1$ , expression (5) of the PSD can be simplified into

$$\Gamma_{\mathbf{k}}(t) \simeq \frac{\sigma_0^2}{4} \exp(2\gamma_{max} t) \exp\left(-\frac{(|\mathbf{k}| - k_{max})^2}{k_t^2}\right),$$

where the spectral width is  $k_t = \sqrt[4]{[(2k_{max}^3)/(3Ag t^2)]}$ . The spectral width of the modulation  $k_t$  decays with time. This gain narrowing effect originates from the fact that the wave numbers close to  $k_{max}$  grow much quicker than the other ones, so that the PSD after a transient period becomes independent of the initial PSD. Of course this holds true only if the initial perturbation contains modulations around  $k_{max}$ , as no new wavelength can be generated during the linear stage.

By collecting the terms of the order of  $\varepsilon^{j+1}$ ,  $j \geq 1$ , in Eq. (3) we obtain a series of linear systems for the  $j$ -order perturbations  $\eta_{\mathbf{k},j}$  and  $\psi_{\mathbf{k},j}$ :

$$\frac{\partial \eta_{\mathbf{k},j}}{\partial t} = L_{\mathbf{k}}^{(0)} \psi_{\mathbf{k},j} + F_{j,1}(\mathbf{k}, (\psi_{\mathbf{k},l}, \eta_{\mathbf{k},l})_{0 \leq l \leq j-1}),$$

$$\frac{\partial \psi_{\mathbf{k},j}}{\partial t} = -G_{\mathbf{k}}^{(0)} \eta_{\mathbf{k},j} + F_{j,2}(\mathbf{k}, (\psi_{\mathbf{k},l}, \eta_{\mathbf{k},l})_{0 \leq l \leq j-1}),$$

where  $F_{j,1}$  and  $F_{j,2}$  are source terms that depend only on  $\eta_{\mathbf{k},l}$  and  $\psi_{\mathbf{k},l}$  for  $l \leq j-1$ . It is consequently possible to solve recursively these systems. At order 3 we get that the Fourier modes can be written as

$$\begin{aligned} \eta_{\mathbf{k}}(t) = & \varepsilon W_0(\mathbf{k}, t) \eta_{\mathbf{k}}(0) \\ & + \frac{\varepsilon^2}{2\pi} \int d^2 \mathbf{k}_0 W_1(\mathbf{k}, \mathbf{k}_0, t) \eta_{\mathbf{k}_0}(0) \eta_{\mathbf{k}-\mathbf{k}_0}(0) \\ & + \frac{\varepsilon^3}{(2\pi)^2} \int \int d^2 \mathbf{k}_0 d^2 \mathbf{k}_1 W_2(\mathbf{k}, \mathbf{k}_0, \mathbf{k}_1, t) \\ & \times \eta_{\mathbf{k}_0}(0) \eta_{\mathbf{k}_1}(0) \eta_{\mathbf{k}-\mathbf{k}_0-\mathbf{k}_1}(0). \end{aligned} \quad (6)$$

Qualitatively, the terms of the order of  $\varepsilon^2$  give the second-order nonlinear corrections. They involve sum-frequency and difference-frequency generations, but the fundamental modulations are not affected at this order. The nonlinear corrections to the fundamental modulations appear in the third-order perturbations in  $\varepsilon^3$ . The full expressions of the  $W_j$ 's are given in Appendix A.

#### IV. SINGLE-MODE PERTURBATION

We consider in this section an initial single-mode perturbation of the interface with carrier wave number  $\mathbf{k}_p$  of forms (1) and (2). At time  $t$  the interface elevation is described by three Fourier modes corresponding to the fundamental, second- and third-harmonic modulations:

$$\begin{aligned} \eta_{\mathbf{k}_p}(t) = & W_0(\mathbf{k}_p, t) \eta_{\mathbf{k}_p}(0) + \frac{1}{(2\pi)^2} [W_2(\mathbf{k}_p, \mathbf{k}_p, \mathbf{k}_p, t) \\ & + W_2(\mathbf{k}_p, -\mathbf{k}_p, \mathbf{k}_p, t) + W_2(\mathbf{k}_p, \mathbf{k}_p, -\mathbf{k}_p, t)] \\ & \times |\eta_{\mathbf{k}_p}(0)|^2 \eta_{\mathbf{k}_p}(0), \\ \eta_{2\mathbf{k}_p}(t) = & \frac{1}{2\pi} W_1(2\mathbf{k}_p, \mathbf{k}_p, t) \eta_{\mathbf{k}_p}(0)^2, \\ \eta_{3\mathbf{k}_p}(t) = & \frac{1}{(2\pi)^2} W_2(3\mathbf{k}_p, \mathbf{k}_p, \mathbf{k}_p, t) \eta_{\mathbf{k}_p}(0)^3. \end{aligned}$$

We also have  $\eta_{-j\mathbf{k}_p}(t) = \eta_{j\mathbf{k}_p}(t)^*$  for  $j=1,2,3$ . The quadratic nonlinear effects induce the first nonlinear correction which consists in the second harmonic generation  $\mathbf{k}_p + \mathbf{k}_p \rightarrow 2\mathbf{k}_p$ . The two other nonlinear corrections originate from cubic and cascaded quadratic effects. They involve third-harmonic generation  $\mathbf{k}_p + \mathbf{k}_p + \mathbf{k}_p \rightarrow 3\mathbf{k}_p$  and self-modulation of the fundamental mode through  $\mathbf{k}_p + \mathbf{k}_p - \mathbf{k}_p \rightarrow \mathbf{k}_p$ . The complete calculations in the absence of surface tension can be found in Ref. [14]. In particular the nonlinear correction to the fundamental modulation is shown to be negative valued which slows down the exponential growth. Let us address the influence of surface tension  $s > 0$ . The expressions become complicated, but they can be simplified if  $\gamma_{\mathbf{k}_p} t \gg 1$  because transient components can be neglected. Further-

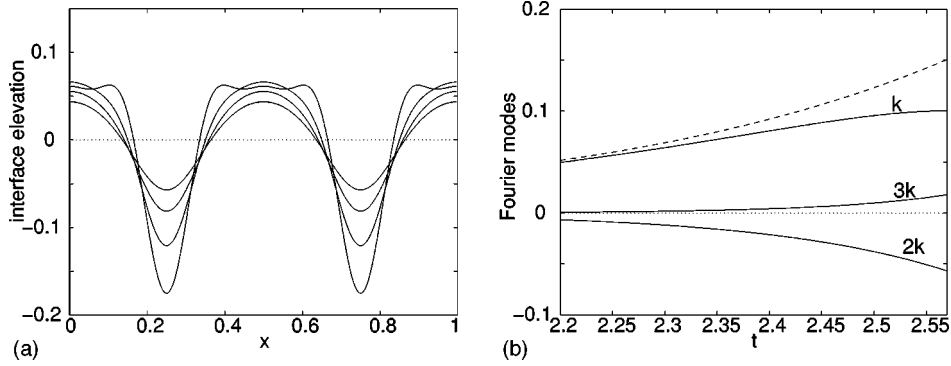


FIG. 1. (a) Evolution of an initial single-mode surface with  $k_p = k_{max} = 2 \times 2\pi$ ,  $\sigma_1 = 10^{-4}$ ,  $A = 1$ ,  $g = 1$ . The graphs correspond to times 2.2, 2.32, 2.45, 2.57 ( $= t_{sat}$ ). (b) Evolutions of the Fourier modes of the three harmonics until the saturation time  $t_{sat}$ . The dashed line corresponds to the exponential growth of the fundamental mode in the linear regime.

more, the gain curve is concave in the sense that  $\gamma_{2k} < 2\gamma_k$  and  $\gamma_{3k} < 3\gamma_k$ . Accordingly we can also neglect components of  $W_j$  which are proportional to  $\exp(\gamma_{2k_p} t)$  [ $\exp(\gamma_{3k_p} t)$ ] with respect to those which are proportional to  $\exp(2\gamma_{k_p} t)$  [ $\exp(3\gamma_{k_p} t)$ ]. We get

$$\begin{aligned} \eta_{k_p}(t) &= (\sqrt{2}\pi) \frac{\sigma_1}{2} \exp(\gamma_{k_p} t) - \frac{\sqrt{2}\pi}{64} \left( \frac{6A^2}{4 - \gamma_{2k_p}^2 / \gamma_{k_p}^2} |\mathbf{k}_p|^2 \right. \\ &\quad \left. + |\mathbf{k}_p|^2 - \frac{3}{16} \frac{|\mathbf{k}_p|^5}{k_{max}^3} \frac{\gamma_{max}^2}{\gamma_{k_p}^2} \right) \exp(3\gamma_{k_p} t) \sigma_1^3, \\ \eta_{2k_p}(t) &= -\pi \frac{A|\mathbf{k}_p|}{2(4 - \gamma_{2k_p}^2 / \gamma_{k_p}^2)} \exp(2\gamma_{k_p} t) \sigma_1^2, \\ \eta_{3k_p}(t) &= \frac{\sqrt{2}\pi}{9 - \gamma_{3k_p}^2 / \gamma_{k_p}^2} \left( \frac{3|\mathbf{k}_p|^2}{2(4 - \gamma_{2k_p}^2 / \gamma_{k_p}^2)} A^2 - \frac{3|\mathbf{k}_p|^2}{16} \right. \\ &\quad \left. - \frac{9}{128} \frac{|\mathbf{k}_p|^5}{k_{max}^3} \frac{\gamma_{max}^2}{\gamma_{k_p}^2} \right) \exp(3\gamma_{k_p} t) \sigma_1^3. \end{aligned}$$

If  $\mathbf{k}_p$  has a modulus close to  $k_{max}$  then

$$\begin{aligned} \eta_{k_p}(t) &= (\sqrt{2}\pi) \frac{\sigma_1}{2} \exp(\gamma_{max} t) \\ &\quad - (\sqrt{2}\pi) \frac{k_{max}^2 \left( \frac{13}{8} + 3A^2 \right)}{128} \exp(3\gamma_{max} t) \sigma_1^3, \\ \eta_{2k_p}(t) &= -(\sqrt{2}\pi) \frac{A k_{max}}{8\sqrt{2}} \exp(2\gamma_{max} t) \sigma_1^2, \\ \eta_{3k_p}(t) &= \frac{(\sqrt{2}\pi) k_{max}^2}{3} \left( \frac{A^2}{8} - \frac{11}{128} \right) \exp(3\gamma_{max} t) \sigma_1^3. \quad (7) \end{aligned}$$

We shall consider that the saturation is effective when the growth of the fundamental Fourier mode is stopped. The saturation time is thus defined by

$$t_{sat} = \inf_{t \geq 0} \left\{ \frac{\partial \Gamma_{k_p}(t)}{\partial t} < 0 \right\}, \quad \Gamma_{k_p}(t) = |\eta_{k_p}(t)|^2.$$

By considering the expression of the mode  $\eta_{k_p}(t)$  we get that the saturation is effective when

$$\eta_{rms}^{lin}(t) k_{max} \frac{\sqrt{13 + 24A^2}}{4\sqrt{2}} \approx 1, \quad (8)$$

where  $\eta_{rms}(t) = \langle \eta^2(t, \mathbf{x}) \rangle^{1/2}$  is the interface elevation rms which is equal in the linear regime to  $\eta_{rms}^{lin}(t) = \sigma_1 \cosh(\gamma_{max} t) \approx \sigma_0 \exp(\gamma_{max} t) / 2$ . At saturation time the expression of the fundamental Fourier mode in the WNL regime is related to the one in the linear regime by  $\eta_{k_p}(t) = (1/\sqrt{2}) \eta_{k_p}(t)|_{lin}$ . Accordingly the saturation condition reads in the more conventional way as:

$$\eta_{rms}^{loc}(t) \approx c_{sat} \lambda_{max}, \quad c_{sat} = \frac{2}{\pi \sqrt{13 + 24A^2}}, \quad (9)$$

where the local elevation rms  $\eta_{rms}^{loc}(t)$  is equal to  $|\eta_{k_p}(t)| / (\sqrt{2}\pi)$  in the single-mode case. For an Atwood number  $A = 1$ , we have  $c_{sat} = 0.105$ , which is in agreement with the values exhibited from numerical simulations (Haan's estimate is  $c_{sat} = 0.1$  [15]).

Most of the numerical simulations are carried out in two dimensional, so we briefly address the case of a 2D single-mode configuration with wave vector  $k_p$ . If  $k_p$  is equal to  $\pm k_{max}$ , then we have the same formulas (7) for the Fourier modes as in the 3D case if we take care to substitute  $\sqrt{\pi}$  for the factors  $\sqrt{2}\pi$ . As shown in Fig. 1, the second- and third-harmonic generations give rise to bubbles and spikes formation. The saturation condition reads in terms of the interface elevation rms in the linear regime as Eq. (8) similarly as in the 3D case. This is not surprising as a single-mode perturbation in three dimensions is not sensitive to one of the transverse spatial variables.

## V. MULTIMODE PERTURBATION

The WNL analysis consists in expanding the interface elevation with respect to its initial amplitude  $\varepsilon \ll 1$ ,

$$\eta_{\mathbf{k}}(t) = \varepsilon \eta_{\mathbf{k},0} + \varepsilon^2 \eta_{\mathbf{k},1} + \varepsilon^3 \eta_{\mathbf{k},2} + O(\varepsilon^4),$$

where  $\eta_{\mathbf{k},j}$  contains terms of the form  $\eta_{\mathbf{k}_0}(0) \dots \eta_{\mathbf{k}_j}(0)$ ,  $\mathbf{k}_0 + \dots + \mathbf{k}_j = \mathbf{k}$ . The physically relevant quantity is the PSD. The second moment of the Fourier modes can be expanded in powers of  $\varepsilon$  and we get

$$\begin{aligned} \langle |\eta_{\mathbf{k}}(t)|^2 \rangle &= \varepsilon^2 \langle |\eta_{\mathbf{k},0}|^2 \rangle + \varepsilon^4 (2 \operatorname{Re} \langle \eta_{\mathbf{k},0}^* \eta_{\mathbf{k},2} \rangle + \langle |\eta_{\mathbf{k},1}|^2 \rangle) \\ &\quad + O(\varepsilon^6). \end{aligned}$$

This equation shows that the lowest-order WNL correction for the PSD is of the order of  $\varepsilon^4$  and depends both on the second- and third-order terms of the WNL expansion. That is why it is necessary to develop a third-order WNL analysis to capture all effects of comparable magnitude in the multimode case. Haan [5] performs a WNL analysis in the multimode case where the term  $2 \operatorname{Re} \langle \eta_{\mathbf{k},0}^* \eta_{\mathbf{k},2} \rangle$  is neglected. This allows us to report on high-frequency generation by sum-frequency, but important phenomena are not captured, such as the saturation of the growth of the fundamental modulations, although this mechanism has the same order of magnitude. This is in dramatic contrast with the single-mode case where the second-harmonic generation is much stronger than the nonlinear feedback on the fundamental modulation.

In the WNL regime the PSD has the following form:

$$\begin{aligned} \Gamma_{\mathbf{k}}(t) &= W_0^2(\mathbf{k}, t) \Gamma_{\mathbf{k}}(0) + \frac{1}{(2\pi)^2} \int d^2 \mathbf{k}_0 W_1(\mathbf{k}, \mathbf{k}_0, t) \\ &\quad \times [W_1(\mathbf{k}, -\mathbf{k}_0, t) + W_1(\mathbf{k}, \mathbf{k}_0 - \mathbf{k}, t)] \Gamma_{\mathbf{k}_0}(0) \Gamma_{\mathbf{k}-\mathbf{k}_0}(0) \\ &\quad + \frac{1}{(2\pi)^2} \int d^2 \mathbf{k}_0 2W_0(\mathbf{k}, t) \\ &\quad \times [W_2(\mathbf{k}, \mathbf{k}, \mathbf{k}_0, t) + W_2(\mathbf{k}, \mathbf{k}_0, \mathbf{k}, t) \\ &\quad + W_2(\mathbf{k}, \mathbf{k}_0, -\mathbf{k}_0, t)] \Gamma_{\mathbf{k}_0}(0) \Gamma_{\mathbf{k}}(0). \end{aligned}$$

Note that in dimension 2 the factors  $1/(2\pi)^2$  should be changed into  $1/(2\pi)$ . The expression of  $W_2$  is easily tractable by a computerized system such as MAPLE, so that it can be integrated and theoretical PSD profiles can be obtained. Another approach consists in deriving approximate expressions that will hold true in case of strong spectral narrowing effects. Let us assume that  $\gamma_{max} t > 1$ . The spectral narrowing effect is then strong, as the modes with wave number around  $k_{max}$  have been growing much more than the other ones during the linear stage. As a result the main WNL contributions originate from coupling  $\mathbf{k}_0 + \mathbf{k}_1 \rightarrow \mathbf{k}$  and  $\mathbf{k}_0 + \mathbf{k}_1 + \mathbf{k}_2 \rightarrow \mathbf{k}$  between modes whose wave numbers  $|\mathbf{k}_j|$  are close to  $k_{max}$ . Furthermore, the gain curve is concave in the sense that  $\gamma_{\mathbf{k}_0 + \mathbf{k}_1} < \gamma_{\mathbf{k}_0} + \gamma_{\mathbf{k}_1}$  and  $\gamma_{\mathbf{k}_0 + \mathbf{k}_1 + \mathbf{k}_2} < \gamma_{\mathbf{k}_0} + \gamma_{\mathbf{k}_1} + \gamma_{\mathbf{k}_2}$ . Accordingly we can neglect terms proportional to  $\exp(\gamma_{\mathbf{k}_0 + \mathbf{k}_1} t)$

$[\exp(\gamma_{\mathbf{k}_0 + \mathbf{k}_1 + \mathbf{k}_2} t)]$  with respect to terms proportional to  $\exp[(\gamma_{\mathbf{k}_0} + \gamma_{\mathbf{k}_1})t]$   $[\exp(\gamma_{\mathbf{k}_0} + \gamma_{\mathbf{k}_1} + \gamma_{\mathbf{k}_2})t]$ . In this framework the expression of  $W_0$  becomes  $W_0(\mathbf{k}, t) = (1/2)\exp(\gamma_{\mathbf{k}} t)$ , the expression of  $W_1$  can be simplified into

$$W_1(\mathbf{k}, \mathbf{k}_0, t) = \frac{1}{4} \frac{\exp[(\gamma_{\mathbf{k}_0} + \gamma_{\mathbf{k}_1})t]}{4 - \gamma_{\mathbf{k}}^2 / \gamma_{max}^2} (Q_{\mathbf{k}_0, \mathbf{k}_1}^{(1)} + P_{\mathbf{k}_0, \mathbf{k}_1}^{(1)}),$$

where  $\mathbf{k}_1 = \mathbf{k} - \mathbf{k}_0$ . Finally, denoting  $\mathbf{k}_2 = \mathbf{k} - \mathbf{k}_0 - \mathbf{k}_1$ , the expression of  $W_2$  can be reduced to

$$\begin{aligned} W_2(\mathbf{k}, \mathbf{k}_0, \mathbf{k}_1, t) &= \frac{1}{8} \frac{\exp[(\gamma_{\mathbf{k}_0} + \gamma_{\mathbf{k}_1} + \gamma_{\mathbf{k}_2})t]}{9 - \gamma_{\mathbf{k}}^2 / \gamma_{max}^2} \left[ \frac{Q_{\mathbf{k}_1, \mathbf{k}_2}^{(1)} + P_{\mathbf{k}_1, \mathbf{k}_2}^{(1)}}{4 - \gamma_{\mathbf{k}_1 + \mathbf{k}_2}^2 / \gamma_{max}^2} \right. \\ &\quad \times (Q_{\mathbf{k}_0, \mathbf{k}_1 + \mathbf{k}_2}^{(1)} + 2P_{\mathbf{k}_0, \mathbf{k}_1 + \mathbf{k}_2}^{(1)}) + \frac{Q_{\mathbf{k}_1, \mathbf{k}_0}^{(1)} + P_{\mathbf{k}_1, \mathbf{k}_0}^{(1)}}{4 - \gamma_{\mathbf{k}_0 + \mathbf{k}_1}^2 / \gamma_{max}^2} \\ &\quad \times (4Q_{\mathbf{k}_0 + \mathbf{k}_1, \mathbf{k}_2}^{(1)} + 2P_{\mathbf{k}_0 + \mathbf{k}_1, \mathbf{k}_2}^{(1)}) + Q_{\mathbf{k}_0, \mathbf{k}_1, \mathbf{k}_2}^{(2)} + P_{\mathbf{k}_0, \mathbf{k}_1, \mathbf{k}_2}^{(2)} \\ &\quad \left. - \frac{|\mathbf{k}|}{8k_{max}^3} (\mathbf{k} \cdot \mathbf{k}_0)(\mathbf{k}_1 \cdot \mathbf{k}_2) \right]. \end{aligned}$$

### A. Mode coupling in dimension 2

In the following we consider the white noise case  $\Gamma_{\mathbf{k}}(0) \equiv \sigma_0^2$ . In the linear regime the PSD is Eq. (5) and the variance of the interface elevation is obtained by integrating the PSD over  $k$ :

$$\eta_{rms}^{lin}(t)^2 := \langle \eta(t, x)^2 \rangle_{lin} \approx \frac{\sigma_0^2 k_t \exp(2\gamma_{max} t)}{4\sqrt{\pi}}. \quad (10)$$

There exist three mechanisms that bring nonlinear corrections to the linear regime with the same order of magnitude. Each mechanism generates a new band of frequencies.

*Low-frequency generation.* By subtracting two wave vectors with wave numbers close to  $k_{max}$  low-frequency modes are generated. It is found that around  $|k| \sim k_t$  the PSD is

$$\Gamma_{\mathbf{k}}(t) \approx \frac{\sigma_0^4 A^2 k_t k^2}{32\sqrt{\pi}} \exp\left(-\frac{k^2}{2k_t^2}\right) \exp(4\gamma_{max} t).$$

This demonstrates the excitation of a low-frequency modulation with typical wave number  $k_b = \sqrt{2}k_t$ .

*High-frequency generation.* By summing two wave vectors with wave numbers close to  $k_{max}$  high-frequency modes with wave numbers around  $2k_{max}$  are generated. More exactly, if  $|k| \sim 2k_{max}$ , then the PSD is

$$\Gamma_{\mathbf{k}}(t) \approx \frac{\sigma_0^4 A^2 k_t k^2}{256\sqrt{2}\sqrt{\pi}} \exp\left(-\frac{(|k| - 2k_{max})^2}{2k_t^2}\right) \exp(4\gamma_{max} t).$$

*Saturation of the growths of the fundamental modulations.* Through nonlinear cubic effects and cascaded quadratic effects, the growths of the fundamental modulations (i.e., those with wave numbers around  $k_{max}$ ) are modified, so that the PSD around  $k_{max}$  reads

$$\Gamma_k(t) \approx \frac{\sigma_0^2}{4} \exp(2\gamma_{max}t) \exp\left(-\frac{(|k| - k_{max})^2}{k_t^2}\right) \times \left[1 - \sigma_0^2 \frac{13 + 24A^2}{128\sqrt{\pi}} k^2 k_t \exp(2\gamma_{max}t)\right].$$

The first term of the right-hand side is the exponential growth of the linear regime, while the second term results from the interplay of all WNL effects. As the second term is always negative valued, this shows that the WNL contribution to the fundamental modulations consists in reducing their exponential growths. This is the phenomenon called WNL saturation.

We shall say that the saturation is effective as soon as the growth of one of the modes is stopped. Accordingly we adopt the following definition of the saturation time:

$$t_{sat} = \inf_{t \geq 0} \left\{ \exists k \text{ such that } \frac{\partial \Gamma_k(t)}{\partial t} < 0 \right\} \quad (11)$$

which is consistent with the one adopted for the single-mode configuration. By considering formula (11) we can see that saturation is effective when

$$k_{max}^2 \langle \eta^2 \rangle_{lin} \frac{13 + 24A^2}{16} \approx 1, \quad (12)$$

where  $\langle \eta^2 \rangle_{lin}$  is given by Eq. (10). The saturation condition (12) is very similar to the one obtained in the single-mode case, up to a factor 2. Roughly speaking the factor 2 originates from the statistical relation  $\langle |\eta_k|^4 \rangle = 2 \langle |\eta_k|^2 \rangle^2$ . As a result saturation is effective for a lower value of the elevation rms in the multimode case than in the single-mode case. Another important feature is that the rms at saturation time decays with the Atwood number as  $1/\sqrt{13 + 24A^2}$ .

The PSD in the WNL regime around  $k_{max}$  is equal to  $\frac{1}{2} \Gamma_k(t)|_{lin}$  at saturation time. If we introduce the local elevation rms  $\eta_{rms}^{loc} = \sqrt{\langle \eta^2 \rangle_{loc}}$ ,

$$\langle \eta^2 \rangle_{loc} := \frac{1}{\pi} \int_{0.75 k_{max}}^{1.25 k_{max}} \Gamma_k(t) dk,$$

then we have at saturation time

$$\eta_{rms}^{loc} \approx c_{sat} \lambda_{max}, \quad c_{sat} = \sqrt{\frac{8}{13 + 24A^2}} \frac{1}{2\pi}. \quad (13)$$

A similar formula has been proposed by Haan [15]. He was the first one to suggest that neighboring modes with similar wavelengths add up to create an effective local amplitude, and that nonlinear saturation should occur when this collective amplitude reaches some value  $c_{sat} \lambda$ . Haan has fixed the

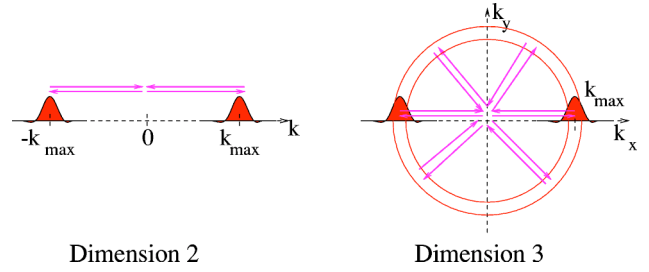


FIG. 2. Difference-frequency generation to create low modes. The possible contributions are plotted and compared in two and three dimensions.

constant  $c_{sat}$  by comparisons with numerical simulations. The literature contains a lot of references for the value of  $c_{sat}$  for an Atwood number  $A = 1$ . In the original paper by Haan the value  $c_{sat} = 0.09$  is proposed, then slightly reduced values can be found in following references [16–18], until the value 0.063 proposed by Ofer *et al.* [11]. The WNL analysis allows us to recover analytically the form of the equation that characterizes nonlinear saturation, as well as the value of the constant  $c_{sat} \approx 0.074$  for  $A = 1$ .

### B. Mode coupling in dimension 3

In this section we consider a 3D white noise case  $\Gamma_{\mathbf{k}}(0) \equiv \sigma_0^2$ . In the linear regime the PSD is Eq. (5) and the variance of the interface elevation is

$$\eta_{rms}^{lin}(t)^2 := \langle \eta(t, \mathbf{x})^2 \rangle_{lin} \approx \frac{\sigma_0^2 k_{max} k_t \exp(2\gamma_{max}t)}{8\sqrt{\pi}}. \quad (14)$$

Mode coupling is more fascinating in dimension 3 than in dimension 2 because of coupling between noncollinear wave vectors. In this section we give the exhaustive list of the mechanisms that bring WNL corrections.

*Low-frequency generation.* Low-frequency generation is more efficient in dimension 3 than in dimension 2 because there exist much more possible combinations of wave vectors that generate small wave numbers (as shown in Fig. 2). As a result, if  $|\mathbf{k}| \sim k_t$  the expression of the PSD is

$$\Gamma_{\mathbf{k}}(t) \approx \frac{\sigma_0^4 A^2}{64\sqrt{2\pi}} \exp(4\gamma_{max}t) k_t k_{max} |\mathbf{k}|^2.$$

*High-frequency generation.* Let us consider the second-harmonic generation. If  $|\mathbf{k}| \sim 2k_{max}$  then the PSD is

$$\Gamma_{\mathbf{k}}(t) \approx \frac{\sigma_0^4 A^2 k_t^{3/2} |\mathbf{k}|^2 k_{max}^{1/2}}{512\Gamma(3/4)\sqrt{\pi} 2^{3/4}} \exp(4\gamma_{max}t) \times \exp\left(-\frac{(|\mathbf{k}| - 2k_{max})^2}{2k_t^2}\right).$$

This expression is very similar to the 2D case. Indeed the generation of a wave vector  $\mathbf{k}$  with modulus close to  $2k_{max}$  by the sum of two wave vectors  $\mathbf{k}_1$  and  $\mathbf{k}_2$  with moduli close to  $k_{max}$  requires a collinear configuration  $\mathbf{k}_1 + \mathbf{k}_2$  (Fig. 3).

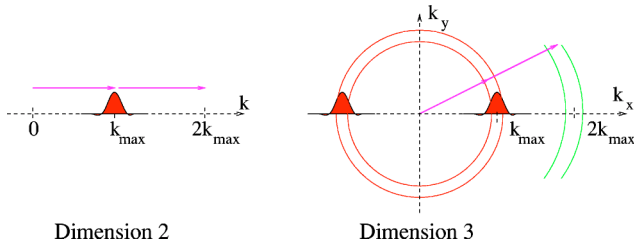


FIG. 3. Sum-frequency generation to create second harmonic modulations at  $2k_{max}$ . Comparison between the configurations in two and three dimensions.

*Filling of the spectral gap between  $k_{max}$  and  $2k_{max}$ .* In dimension 3 the high-frequency generation is not reduced to the generation of a second-harmonic modulation as in dimension 2. Indeed noncollinear configurations are possible (Fig. 4). As a result, we could expect a filling of the spectral gap between  $k_{max}$  and  $2k_{max}$  observed in dimension 2. We can observe in the examples that will be treated in the following sections a slight filling, but it is less important than expected *a priori*. The conversion efficiency for the noncollinear configuration described in Fig. 4(a) is actually rather low, which involves the poor filling of the spectral gap between  $k_{max}$  and  $2k_{max}$ . More exactly, if the wave number  $|\mathbf{k}|$  is between  $k_{max}$  and  $2k_{max}$ , then the PSD is

$$\Gamma_{\mathbf{k}}(t) \simeq \frac{\sigma_0^4 A^2 k_t^2 k_{max} |\mathbf{k}|}{256\pi} \exp(4\gamma_{max} t) \times \frac{[2 - |\mathbf{k}|/k_{max} - |\mathbf{k}|^2/(4k_{max}^2)]^2}{\sqrt{1 - |\mathbf{k}|^2/(4k_{max}^2)} [1 - \gamma_{\mathbf{k}}^2/(4\gamma_{max}^2)]}.$$

Note that the conversion efficiency is roughly proportional to the function  $k \mapsto [2 - k/k_{max} - k^2/(4k_{max}^2)]^2$ . This function has a minimum close to  $(3/2)k_{max}$ , which explains the poor filling of the spectral gap.

*Filling of the spectral gap between 0 and  $k_{max}$ .* The low-frequency generation in dimension 3 does not reduce to the generation of “ $0k_{max}$ ” modulations as in dimension 2. Noncollinear configurations are possible (Fig. 4). We can thus expect a filling of the spectral gap between 0 and  $k_{max}$  observed in dimension 2. In this case (contrarily to the spectral gap between  $k_{max}$  and  $2k_{max}$ ) this filling is quite important because the conversion efficiency for the noncollinear configurations presented in Fig. 4(b) is high. As a result, if the wave number  $|\mathbf{k}|$  is between 0 and  $k_{max}$ , then the PSD is

$$\Gamma_{\mathbf{k}}(t) \simeq \frac{\sigma_0^4 A^2 k_t^2 k_{max} |\mathbf{k}|}{256\pi} \exp(4\gamma_{max} t) \times \frac{[2 - |\mathbf{k}|/k_{max} - |\mathbf{k}|^2/(4k_{max}^2)]^2}{\sqrt{1 - |\mathbf{k}|^2/(4k_{max}^2)} [1 - \gamma_{\mathbf{k}}^2/(4\gamma_{max}^2)]}.$$

Note that the frequency conversion efficiency is roughly proportional to the function  $k \mapsto [2 - k/k_{max} - k^2/(4k_{max}^2)]^2$ . This function has a maximum close to  $(1/2)k_{max}$ , which explains the good filling of the spectral gap.

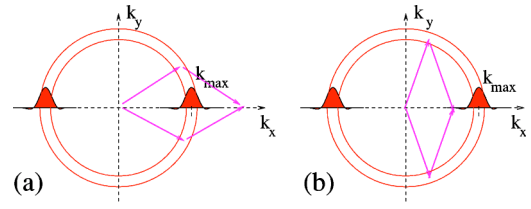


FIG. 4. Sum of frequencies in noncollinear configurations.

*Saturation of the growths of the fundamental modulations.* Nonlinear corrections to the exponential growth of the fundamental modes are built up through cubic and cascaded quadratic effects. These corrections are stronger than in dimension 2 due to contributions from noncollinear wave vectors configurations (see Fig. 5). Taking into account all possible configurations, we get that if  $|\mathbf{k}| \simeq k_{max}$ , then the PSD is

$$\Gamma_{\mathbf{k}}(t) \simeq \frac{\sigma_0^2}{4} \exp(2\gamma_{max} t) \exp\left(-\frac{(|\mathbf{k}| - k_{max})^2}{k_t^2}\right) \times \left[1 - \sigma_0^2 \frac{\alpha(A) k_t k_{max} |\mathbf{k}|^2}{16\sqrt{\pi}} \exp(2\gamma_{max} t)\right],$$

where  $\alpha(A) = 0.518A^2 + 0.573$  [ $\alpha(A=1) = 1.090$ ].

We adopt the same definition of the saturation time than in dimension 2. By considering formula (15), we get that saturation is effective when

$$k_{max}^2 \langle \eta^2 \rangle_{lin} \alpha(A) \simeq 1, \quad (15)$$

where  $\langle \eta^2 \rangle_{lin}$  is given by Eq. (14). This condition looks like very similar as the corresponding one [Eq. (12)] in dimension 2, up to a multiplicative constant. By comparing the values of the constant we get that, for a given  $k_{max}$ , the interface elevation rms saturates at a higher level in dimen-

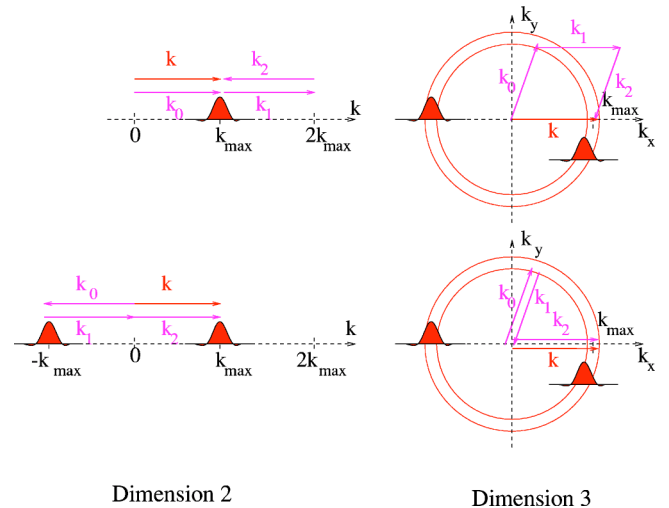


FIG. 5. Nonlinear correction to the fundamental modulations by summation of three wave vectors  $\mathbf{k}_0$ ,  $\mathbf{k}_1$ , and  $\mathbf{k}_2$  (with modulus  $\sim k_{max}$ ). One of these three wave vectors is equal to  $\mathbf{k}$ , the other two ones are complementary.

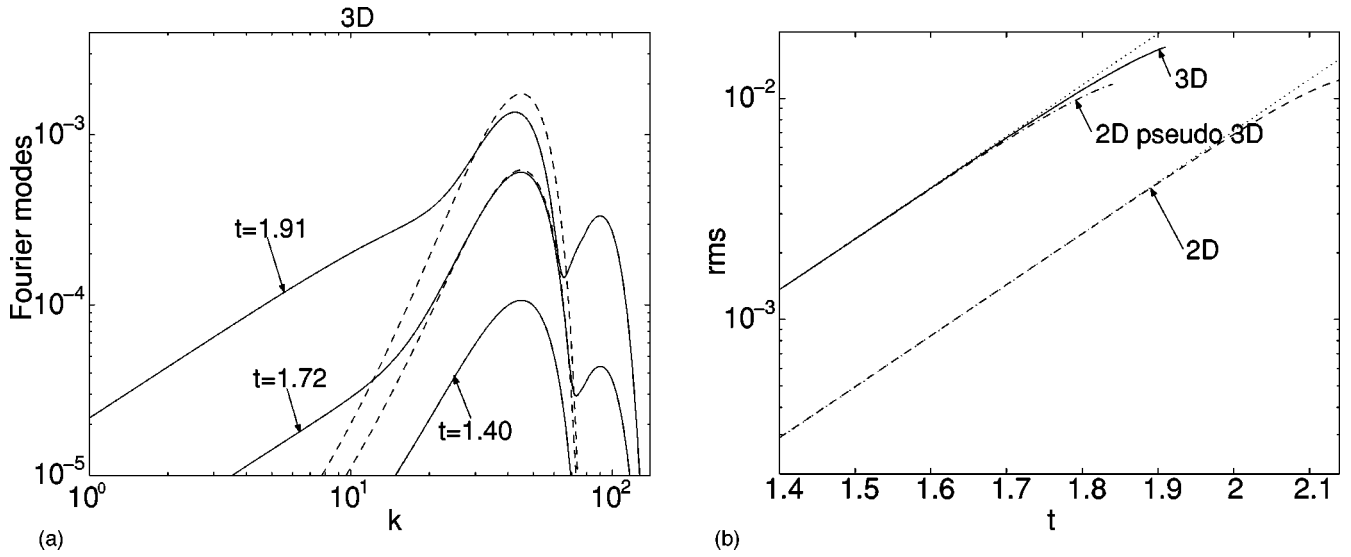


FIG. 6. Evolution of the interface. (a) Fourier modes (square root of the PSD) plotted at different times in the 3D case. The last time is  $t_{sat}$ . Here  $k_{max}=45$  in dimensionless units. The initial perturbation is a white noise with  $\sigma_0=10^{-7}$ . The dashed lines correspond to the exponential growths of the linear regime, the solid lines correspond to the WNL regime. (b) plots the growth of the rms in time. The dotted lines also correspond to the linear regime.

sion 3 than in dimension 2. More precisely, if we introduce the local elevation rms  $\eta_{rms}^{loc} = \sqrt{\langle \eta^2 \rangle_{loc}}$ ,

$$\langle \eta^2 \rangle_{loc} := \frac{1}{2\pi} \int_{0.75 k_{max}}^{1.25 k_{max}} \Gamma_k(t) k dk,$$

then we can express the saturation condition as

$$\eta_{rms}^{loc} \approx c_{sat} \lambda_{max}, \quad c_{sat} = (40.9A^2 + 45.2)^{-1/2}. \quad (16)$$

## VI. ROLE OF THE INITIAL SPECTRUM

### A. White noise spectrum

The aim of this section is to carefully analyze the WNL regime for a white noise perturbation and to discuss the influence of the dimension of the problem. This problem is practically relevant because most of the numerical simulations are carried out in two dimensions and their relevance to physical 3D situations is questionable. In the 2D case the initial PSD is  $\Gamma_k(0)|_{2D} = \sigma_0^2$  and in the 3D case  $\Gamma_k(0)|_{3D} = \sigma_0^2$ . We would also like to consider a 2D-pseudo-3D configuration, which is a configuration in two dimensions with a PSD that corresponds to a 3D white noise. The corresponding 2D-pseudo-3D spectrum is not white, but it is linearly enhanced for the high modes:  $\Gamma_k(0)|_{2D-pseudo-3D} = \sigma_0^2 |k|/2$ . This configuration has recently been proposed to enhance the relevance of the results of 2D numerical simulations to 3D realistic situations.

The dynamics is analyzed until the saturation time. We denote by  $k_{sat}$  the wave number of the mode that saturates first. In the white noise case, it is very close to  $k_{max}$ , actually slightly above. All the following results have been computed in the framework  $A=1$  and  $g=1$ . We have found that the 2D and 2D-pseudo-3D cases are almost identical. The only difference stands in the fact that the saturation occurs earlier

in the 2D-pseudo-3D case, because the initial Fourier modes around  $k_{max}$  have stronger amplitudes in the 2D-pseudo-3D case than in the 2D case. At saturation time, the PSD and the rms are very similar for the 2D and 2D-pseudo-3D cases, and very different from the PSD of the 3D case. We can see in Fig. 6 that the rms computed in the linear regime at saturation time in the 2D and 2D-pseudo-3D cases are the same and satisfy  $\eta_{rms}^{lin} k_{sat} = \sqrt{16/37} \approx 0.65$ . In the same conditions the rms in the 3D case is higher,  $\eta_{rms}^{lin} k_{sat} \approx 0.96$ .

The rms  $\eta_{rms}$  computed in the WNL regime is obtained by integrating the WNL PSD over frequency. At saturation time the WNL rms is below the linear rms because the growths of the dominant modes have been slowed down. We find that the product  $\eta_{rms} k_{sat} \approx 0.53$  at saturation time in dimension 2, while we have  $\eta_{rms} k_{sat} \approx 0.78$  in dimension 3. Finally, if we integrate the PSD over the nearby wave numbers of  $k_{max}$ , then we get the values of  $\eta_{rms}^{loc} k_{max}$  exhibited here above [formulas (13)–(16)]. This study demonstrates that the extrapolations of results of 2D simulations to 3D realistic configurations are not easy, even if we take care to consider a 2D initial spectrum which has a 3D behavior.

### B. Algebraic spectrum

The white noise case studied in the preceding section is usually not encountered in realistic configurations. Indeed available experimental data show that the initial perturbation is a colored noise [9,19]. We assume here that the initial spectrum has power law decay:

$$\Gamma_k(0) = \frac{\sigma^2}{(1 + |\mathbf{k}|^p/k_c^p)^2}.$$

Two different types of behaviors can be encountered.

If the amplitude of the initial perturbation is weak [Fig.

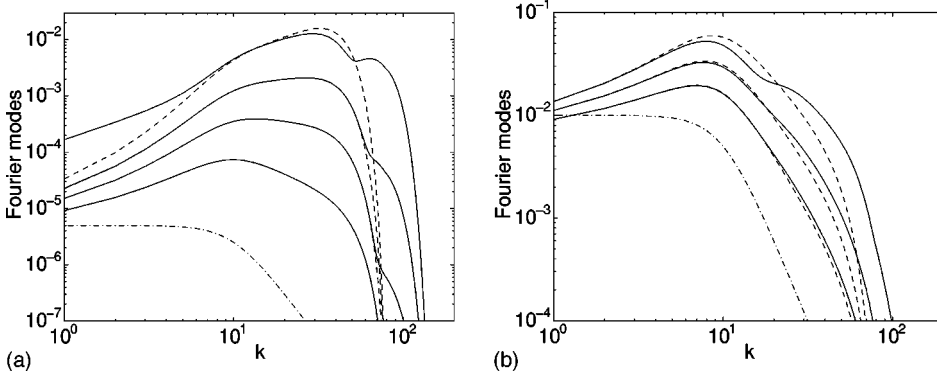


FIG. 7. Fourier modes (square root of the PSD) plotted at different times. 2D configuration with  $k_{max} = 45$ . The initial spectrum (in dot-dashed lines) is algebraic with  $k_c = 10$ ,  $p = 4$ , and  $\sigma = 5 \times 10^{-6}$  (a),  $\sigma = 10^{-2}$  (b). The dashed lines correspond to the exponential growths of the linear regime; the solid lines correspond to the WNL regime.

7(a)], then the linear regime will last long enough so that the spectral gain selection will prevail. This results in a loss of memory of initial conditions which is known to occur in these systems [10]. Accordingly the dominant modes will be those with wave numbers around  $k_{max}$  and the results are very similar to the white noise case: (1) Saturation of the exponential growths of the modes occurs first for the modes around  $k_{max}$ ; (2) the low-frequency modes are enhanced by mode coupling from the dominant modes; (3) high frequencies are also generated by mode coupling.

If the initial perturbation of the interface elevation is strong [Fig. 7(b)], then some low-frequency modes will reach amplitudes that excite WNL effects before the modes around  $k_{max}$ . Saturation happens earlier than the saturation time computed in the preceding section (see the discussion below). The occurrence of such an event requires that the amplitudes of the low-frequency modes of the initial perturbation are high enough. In such a case we have the following.

(1) The modes corresponding to high-frequency modulations, included those around  $k_{max}$ , are imposed by cascaded sum-frequency generations from the low-frequency modes, and not by the exponential growths of the initial modes.

(2) Saturation occurs first for the modes around  $k_c$ .

(3) The Fourier modes below  $k_c$  grow exponentially with their respective linear growth rates. They are not affected by mode coupling from modes around  $k_c$ . This case is thus very different from the white noise case.

It is not easy to quantify analytically the threshold value of the initial rms that leads to one or the other behaviors described here, because we deal with a competition between polynomial terms and exponential of polynomials. But of course this can be done with the help of a software such as MAPLE, as for instance in Fig. 7(b). Besides it is possible to describe precisely the initial dynamics of the low modes in the linear stage. Let  $c_p = (2p - 1)^{1/p}$  and  $f$  be the function defined over  $(0, c_p]$  by  $f(c) = c^{1/2-p} + c^{1/2}$ . We introduce the critical time  $t_{disp} = (2p - 1)^{1 - 1/(2p)} / \sqrt{Agk_c}$ . If  $t \leq t_{disp}$ , then there exists a maximum of the PSD at

$$k_b(t) = k_c f^{-1} \left( \frac{2p}{\sqrt{Agk_c t}} \right),$$

where  $f^{-1}$  is the inverse function of  $f$ . At time  $t_{disp}$ , this wave number is  $k_b(t_{disp}) = c_p k_c$  (this holds true if at time

$t_{disp}$  the linear regime is still valid). If  $t > t_{disp}$ , there is no more maximum of the PSD in the low modes, but only around  $k_{max}$ . Accordingly, until time  $t_{disp}$  we must consider the band of modes around  $k_b(t)$  and the one around  $k_{max}$  to decide whether the linear stage has ended up. This is done by computing  $\eta_{rms}^b$ , the sum of the modes around  $k_b(t)$ , and  $\eta_{rms}^h$ , the sum of the modes around  $k_{max}$ ; we enter the WNL regime as soon as either  $\eta_{rms}^b k_b$  or  $\eta_{rms}^h k_{max}$  reaches the critical value 0.53 (dimension 2) or 0.78 (dimension 3). The first product to reach the critical value indicates which modes saturate first. If such an event has not occurred before  $t_{disp}$ , then, after  $t_{disp}$ , the modes around  $k_{max}$  grow up exponentially fast and we get back a configuration very similar to the white noise case.

We now apply our results to a typical RT situation: Read and Young's rocket rig experiment (experiment 35 [9]). This is a 3D configuration where the initial interface perturbation has very low amplitude so that the spectral selection induced by the gain curve is expected to be strong. Accordingly the precise description of the initial spectrum is not very important. We may think at different sources of perturbation (vibrational noise, . . .) and thermal noise is certainly a lower bound. Following Ref. [5], we use thermal excitations for the initial perturbation

$$\Gamma_{\mathbf{k}}(0) = \frac{k_B T_0}{g_0(\rho_h - \rho_l) + s|\mathbf{k}|^2},$$

where  $k_B = 1.28 \times 10^{-23}$  J/K is the Boltzmann constant,  $T_0 \approx 300$  K is the room temperature,  $g_0 = 9.8$  m/s<sup>2</sup> is the stable acceleration of gravity before the experiment,  $\rho_h = 1.88$  g/cm<sup>3</sup>,  $\rho_l = 0.63$  g/cm<sup>3</sup>,  $g = 304$  m/s<sup>2</sup> is the experimental acceleration, and  $s = 36$  dyn/cm is the surface tension. Here the gain curve is maximal for  $k_{max} \approx 19$  cm<sup>-1</sup>, and Fig. 8(a) confirms that the spectral selection succeeds in driving up this mode and that saturation first occurs for this wave number. Note that the Atwood number  $A = 0.5$ , so that the product  $\eta_{rms} k_{sat} \approx 1.2$  at saturation time [see Fig. 8(b)].

### C. Exponential spectrum

It is not an easy task to derive closed-form expressions for the first saturating mode or the saturation time in the case of algebraic spectra, because we had to deal with competition between polynomials and exponential of polynomials in the

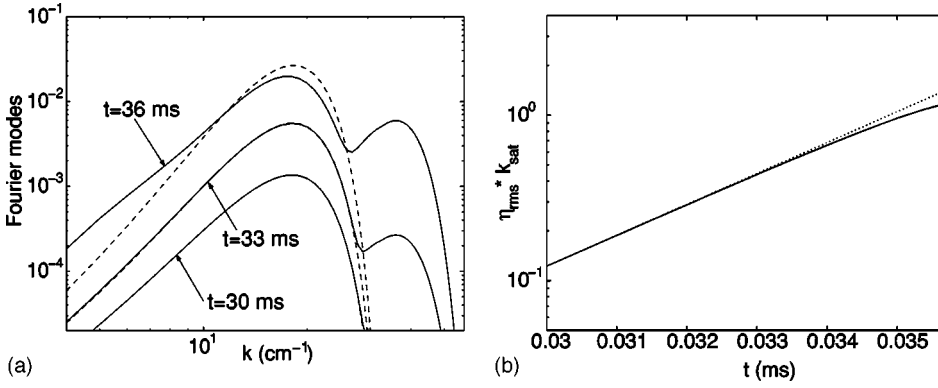


FIG. 8. Fourier modes (square roots of the PSD) plotted at different times for Read and Youngs's rocket rig experiment (a). The product  $\eta_{rms} k_{sat}$  is plotted in (b) (solid line) and compared with the exponential growth of the linear regime (dotted line).

expression of the PSD. Here we consider a different type of colored noise, with an exponentially decaying spectrum

$$\Gamma_{\mathbf{k}}(0) = \sigma^2 \exp(-|\mathbf{k}|/k_c).$$

If  $k_c \rightarrow \infty$  then we get the white noise case. If  $k_c$  is small, then the initial spectrum decays very fast so that low modes are initially dominant, and the high modes will be progressively enhanced by the spectral gain.

The choice of  $k_c$  (i.e., the exponential decay of the initial spectrum) imposes the selection of the wave number that will saturate first. Indeed, the spectrum decays exponentially, while the gain factor is an exponential function of  $|\mathbf{k}|$  with entries that grow up with time. Accordingly the wave number of the dominant mode of the elevation interface increases continuously in time from  $k_c$  to  $k_{max}$ , and does not experience the sharp transition that we have seen in the case of an algebraic spectrum.

The wave number of the dominant mode can be computed analytically. Let  $\phi$  be the function defined over  $[0,1]$  by  $\phi(x) = \sqrt{x(1-x^2/3)}/(1-x^2)$ . The wave number of the dominant mode is

$$k_p(t) = k_{max} \phi^{-1} \left( \frac{k_c \sqrt{Ag t}}{\sqrt{k_{max}}} \right).$$

If  $k_c^2 Ag t \ll k_{max}$ , then we have  $k_p(t) \approx k_c^2 Ag t^2$ . If  $k_c^2 Ag t \gg k_{max}$ , then  $k_p(t) \approx k_{max}$ . We plot in Figs. 9 the evolution

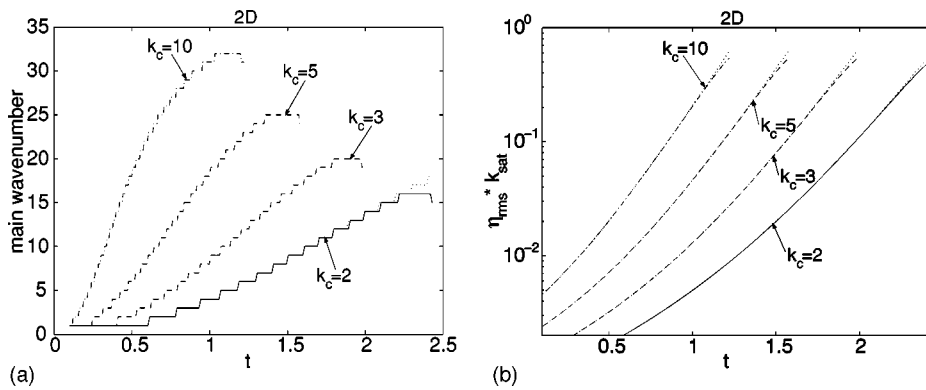


FIG. 9. RT instability dynamics. Here we have  $k_{max} = 45$ . The initial spectrum is exponentially decaying with  $\sigma = 10^{-4}$  and we consider different values for the decay rate  $k_c$ . (a) plots the wave number of the dominant mode as a function of time. (b) plots the product  $\eta_{rms} k_{sat}$  which saturates at a value independent of  $k_c$ . In (b) the dotted lines correspond to the exponential growths of the linear regime.

of the interface elevation until the saturation time for different values of  $k_c$ . By choosing  $k_c$  we can select the wave number  $k_{sat}$  as shown by Fig. 9(a). For instance, if  $k_c = 2$ , then  $k_{sat} = 15$ , while for  $k_c = 10$  we get  $k_{sat} = 31$ . We also get that the rms at saturation time is a function of  $k_c$ , but the important point is that the product  $\eta_{rms}^{lin} k_{sat}$  at saturation time is a constant that depends only on the dimension and the Atwood number. For dimension 2 and  $A = 1$ , we have at saturation time  $\eta_{rms}^{lin} k_{sat} = \sqrt{16/37} \approx 0.65$  as shown by Fig. 9(b).

## VII. CONCLUSION

To sum up, a weakly nonlinear model has been proposed to study the Rayleigh-Taylor instability in the presence of surface tension. This model addresses the case of an initial multimode perturbation and uses statistical analysis. We show that the computation of the third-order nonlinearity is necessary and sufficient to capture the nonlinear saturation of the growth of the interface modulation. This contribution allows us to justify the saturation condition first introduced by Haan [5,15].

The linear regime is characterized by the exponential growths of the Fourier modes of the initial spectrum. The gain curve has a maximum at wave number  $k_{max}$  and can be fitted by a Gaussian function centered at  $k_{max}$  with width  $k_t \sim k_{max}^{3/4}/(Ag t^2)^{1/4}$ . Consequently, if the initial spectrum is a

white noise, then the linear stage of the dynamics will drive up the modulations around  $k_{max}$ . This phenomenon is called spectral gain narrowing. When the amplitude of the interface modulation becomes strong enough, nonlinear effects involve mode coupling between the surface modes. In the early stage of the nonlinear dynamics only quadratic and cubic effects are important which corresponds to the weakly nonlinear stage characterized by the following mechanisms: (1) High-frequency generation by sum frequency, (2) low-frequency generation by difference frequency, (3) saturation of the exponential growths of the dominant modes around  $k_{max}$ . Saturation is effective as soon as the product  $k_{max}\eta_{rms}^{loc}(t)$  reaches a critical value that depends only on the dimension and the Atwood number.

Some of these results can be generalized to colored noises, but original features appear. The modes around  $k_{max}$  are not always the ones that saturate first. It is not possible to separate the study of RT instabilities into the analysis of the low-frequency modes on the one hand and of high-frequency modes on the other hand. If the initial amplitudes of the low-frequency modes are strong enough, then cascaded nonlinear mode coupling of the low-frequency modes will bring the main contribution to the growth of the high-frequency modes. Inversely, if the high-frequency modes are strongly amplified by the linear stage, then they will drive up the low-frequency dynamics by difference-frequency mechanisms.

Nevertheless, we have exhibited an important feature that does not depend on the initial spectrum. The ratio  $\eta_{rms}^{loc}/\lambda_{sat}$  at saturation time is a function that depends only on the dimension of the system and the Atwood number. If  $A=1$ , then in dimension 2,  $\eta_{rms}^{loc} \approx 0.074\lambda_{sat}$  and in dimension 3 we have  $\eta_{rms}^{loc} \approx 0.108\lambda_{sat}$ . This remark may help to understand, for instance, the phenomenological model based on the so-called wavelength renormalization hypothesis (WRH) first introduced by Belenkii and Fradkin [20], discussed in Refs. [10,21–23], and developed in a systematic way by Ramshaw [24]. The WRH suggests that the interface behaves as if it always remains in the linear regime, but with a time-dependent wavelength which is continuously dynamically renormalized to a value of the order of the interface rms. Accordingly the ANSATZ  $\eta_{rms} = c/\lambda$  (where  $c$  is a well-chosen constant) is substituted into the single-mode linear evolution equation to study the multimode nonlinear dynamics.

#### ACKNOWLEDGMENT

We thank Pierre-Arnaud Raviart for useful and stimulating discussions.

#### APPENDIX: $W_j$ COEFFICIENTS

The following expressions extend the formulas given in Ref. [14] in the absence of surface tension. The entries of the expansion of the Hamiltonian are  $G_{\mathbf{k}}^{(0)} = (\rho_2 - \rho_1)g + s|\mathbf{k}|^2$ ,  $G_{\mathbf{k},\mathbf{k}_0}^{(1)} = 0$ ,  $G_{\mathbf{k},\mathbf{k}_0,\mathbf{k}_1}^{(2)} = (s/4)(\mathbf{k} \cdot \mathbf{k}_0)(\mathbf{k}_1 \cdot \mathbf{k}_2)$ ,

$$L_{\mathbf{k}}^{(0)} = \frac{|\mathbf{k}|}{\rho_1 + \rho_2},$$

$$L_{\mathbf{k},\mathbf{k}_0}^{(1)} = \frac{A}{\rho_1 + \rho_2} (|\mathbf{k}||\mathbf{k}_0| - \mathbf{k} \cdot \mathbf{k}_0),$$

$$L_{\mathbf{k},\mathbf{k}_0,\mathbf{k}_1}^{(2)} = \frac{1}{\rho_1 + \rho_2} \mathbf{k} \cdot \left( \frac{(\mathbf{k}_0 + \mathbf{k}_1)(\mathbf{k}_0 + \mathbf{k}_1)}{|\mathbf{k}_0 + \mathbf{k}_1|} + \frac{(\mathbf{k}_0 + \mathbf{k}_2)(\mathbf{k}_0 + \mathbf{k}_2)}{|\mathbf{k}_0 + \mathbf{k}_2|} - |\mathbf{k}| - |\mathbf{k}_0| \right) \cdot \mathbf{k}_0,$$

where  $\mathbf{k}_2 = \mathbf{k} - \mathbf{k}_0 - \mathbf{k}_1$ ;

$$P_{\mathbf{k}_0,\mathbf{k}_1}^{(1)} = \frac{L_{\mathbf{k}_0+\mathbf{k}_1,\mathbf{k}_0}^{(1)}}{2L_{\mathbf{k}_0}^{(0)}} + \frac{L_{\mathbf{k}_0+\mathbf{k}_1,\mathbf{k}_1}^{(1)}}{2L_{\mathbf{k}_1}^{(0)}} - \frac{L_{-\mathbf{k}_0,\mathbf{k}_1}^{(1)}L_{\mathbf{k}_0+\mathbf{k}_1}^{(0)}}{2L_{\mathbf{k}_0}^{(0)}L_{\mathbf{k}_1}^{(0)}},$$

$$Q_{\mathbf{k}_0,\mathbf{k}_1}^{(1)} = \frac{L_{\mathbf{k}_0+\mathbf{k}_1,\mathbf{k}_0}^{(1)}}{L_{\mathbf{k}_0}^{(0)}},$$

$$P_{\mathbf{k}_0,\mathbf{k}_1,\mathbf{k}_2}^{(2)} = \frac{L_{\mathbf{k},\mathbf{k}_0,\mathbf{k}_1}^{(2)}}{L_{\mathbf{k}_0}^{(0)}} - \frac{L_{\mathbf{k}}^{(0)}L_{-\mathbf{k}_0,\mathbf{k}_1,\mathbf{k}_2}^{(2)}}{2L_{\mathbf{k}_0}^{(0)}L_{\mathbf{k}_1}^{(0)}},$$

$$Q_{\mathbf{k}_0,\mathbf{k}_1,\mathbf{k}_2}^{(2)} = \frac{L_{\mathbf{k},\mathbf{k}_2,\mathbf{k}_1}^{(2)}}{2L_{\mathbf{k}_2}^{(0)}},$$

$$R_{\mathbf{k}_0,\mathbf{k}_1,\mathbf{k}_2}^{(2)} = -\frac{s}{4}L_{\mathbf{k}}^{(0)}(\mathbf{k} \cdot \mathbf{k}_0)(\mathbf{k}_1 \cdot \mathbf{k}_2),$$

where  $\mathbf{k} = \mathbf{k}_0 + \mathbf{k}_1 + \mathbf{k}_2$ . The coefficients  $W_j$  can be expressed as  $W_0(\mathbf{k}, t) = \cosh(\gamma_{\mathbf{k}} t)$ ,

$$W_1(\mathbf{k}, \mathbf{k}_0, t) = \sum_{j=0}^1 V_1^{(j)}(\mathbf{k}_0, \mathbf{k}_1) \times \frac{\cosh[(\gamma_{\mathbf{k}_0} + \delta_j \gamma_{\mathbf{k}_1})t] - \cosh[\gamma_{\mathbf{k}} t]}{(\gamma_{\mathbf{k}_0} + \delta_j \gamma_{\mathbf{k}_1})^2 - \gamma_{\mathbf{k}}^2},$$

where  $\mathbf{k}_1 = \mathbf{k} - \mathbf{k}_0$ ,  $\delta_j = (-1)^j$ , and

$$V_1^{(j)}(\mathbf{k}_0, \mathbf{k}_1) = \frac{1}{2}(\gamma_{\mathbf{k}_0}^2 Q_{\mathbf{k}_0,\mathbf{k}_1}^{(1)} + \delta_j \gamma_{\mathbf{k}_0} \gamma_{\mathbf{k}_1} P_{\mathbf{k}_0,\mathbf{k}_1}^{(1)}).$$

Finally, denoting  $\mathbf{k}_2 = \mathbf{k} - \mathbf{k}_0 - \mathbf{k}_1$ ,

$$\begin{aligned}
W_2(\mathbf{k}, \mathbf{k}_0, \mathbf{k}_1, t) &= \sum_{j,l=0}^1 V_2^{(jl)}(\mathbf{k}_0, \mathbf{k}_1, \mathbf{k}_2) \frac{\cosh[(\delta_j \gamma_{\mathbf{k}_0} + \delta_l \gamma_{\mathbf{k}_1} + \gamma_{\mathbf{k}_2})t] - \cosh[\gamma_{\mathbf{k}} t]}{(\delta_j \gamma_{\mathbf{k}_0} + \delta_l \gamma_{\mathbf{k}_1} + \gamma_{\mathbf{k}_2})^2 - \gamma_{\mathbf{k}}^2} - \left( \frac{V_1^{(0)}(\mathbf{k}_1, \mathbf{k}_2)}{(\gamma_{\mathbf{k}_1} + \gamma_{\mathbf{k}_2})^2 - \gamma_{\mathbf{k}_1 + \mathbf{k}_2}^2} \right. \\
&\quad \left. + \frac{V_1^{(1)}(\mathbf{k}_1, \mathbf{k}_2)}{(\gamma_{\mathbf{k}_1} - \gamma_{\mathbf{k}_2})^2 - \gamma_{\mathbf{k}_1 + \mathbf{k}_2}^2} \right) W_1(\mathbf{k}, \mathbf{k}_0, t) - \left( \frac{V_1^{(0)}(\mathbf{k}_1, \mathbf{k}_0)}{(\gamma_{\mathbf{k}_0} + \gamma_{\mathbf{k}_1})^2 - \gamma_{\mathbf{k}_0 + \mathbf{k}_1}^2} + \frac{V_1^{(1)}(\mathbf{k}_1, \mathbf{k}_0)}{(\gamma_{\mathbf{k}_0} - \gamma_{\mathbf{k}_1})^2 - \gamma_{\mathbf{k}_0 + \mathbf{k}_1}^2} \right) \\
&\quad \times W_1(\mathbf{k}, \mathbf{k}_0 + \mathbf{k}_1, t), \\
V_2^{(jl)}(\mathbf{k}_0, \mathbf{k}_1, \mathbf{k}_2) &= \frac{1}{2} \left\{ \frac{V_1^{(j)}(\mathbf{k}_1, \mathbf{k}_2)}{(\gamma_{\mathbf{k}_1} + \delta_j \gamma_{\mathbf{k}_2})^2 - \gamma_{\mathbf{k}_1 + \mathbf{k}_2}^2} [\gamma_{\mathbf{k}_0}^2 Q_{\mathbf{k}_0, \mathbf{k}_1 + \mathbf{k}_2}^{(1)} + \delta_j \gamma_{\mathbf{k}_0} (\gamma_{\mathbf{k}_2} + \delta_l \gamma_{\mathbf{k}_1}) P_{\mathbf{k}_0, \mathbf{k}_1 + \mathbf{k}_2}^{(1)}] \right. \\
&\quad + \frac{V_1^{(j+l)}(\mathbf{k}_1, \mathbf{k}_0)}{(\gamma_{\mathbf{k}_0} + \delta_j \delta_l \gamma_{\mathbf{k}_1})^2 - \gamma_{\mathbf{k}_0 + \mathbf{k}_1}^2} [(\gamma_{\mathbf{k}_0} + \delta_j \delta_l \gamma_{\mathbf{k}_1})^2 Q_{\mathbf{k}_0 + \mathbf{k}_1, \mathbf{k}_2}^{(1)} + \delta_j \gamma_{\mathbf{k}_2} (\gamma_{\mathbf{k}_0} + \delta_j \delta_l \gamma_{\mathbf{k}_1}) P_{\mathbf{k}_0 + \mathbf{k}_1, \mathbf{k}_2}^{(1)}] \\
&\quad \left. + \frac{1}{2} (\gamma_{\mathbf{k}_2}^2 Q_{\mathbf{k}_0, \mathbf{k}_1, \mathbf{k}_2}^{(2)} + \delta_j \delta_l \gamma_{\mathbf{k}_0} \gamma_{\mathbf{k}_1} P_{\mathbf{k}_0, \mathbf{k}_1, \mathbf{k}_2}^{(2)} + R_{\mathbf{k}_0, \mathbf{k}_1, \mathbf{k}_2}^{(2)}) \right\}.
\end{aligned}$$

Note that there are two contributions of the surface tension in the expressions of the  $W_j$ . The first contribution to  $W_0$  impedes the linear growth, while the second contribution to  $W_2$  involves a slight reduction of the nonlinear correction to the fundamental modulations as well as a slight reduction of the third-harmonic generation efficiency.

- 
- [1] L. Rayleigh, Proc. London Math. Soc. **14**, 170 (1883).  
[2] S. Chandrasekhar, *Hydrodynamic and Hydromagnetic Stability* (Oxford University Press, London, 1968).  
[3] T. Matsuda, K. Monoto, and T. Shigeyama, *Astrophys. J.* **368**, L27 (1991).  
[4] J.D. Lindl, *Inertial Confinement Fusion* (Springer, New York, 1998).  
[5] S.W. Haan, *Phys. Fluids B* **3**, 2349 (1991).  
[6] S.E. Bodner, *Phys. Rev. Lett.* **33**, 761 (1974).  
[7] T. Ikegawa and K. Nishihara, *Phys. Rev. Lett.* **89**, 115001 (2002).  
[8] T. Ikegawa and K. Nishihara, *Phys. Rev. E* **67**, 026404 (2003).  
[9] K.I. Read, *Physica D* **12**, 45 (1984).  
[10] D.L. Youngs, *Physica D* **12**, 32 (1984).  
[11] D. Ofer, U. Alon, D. Shvarts, R.L. McCrory, and C.P. Verdon, *Phys. Plasmas* **3**, 3073 (1996).  
[12] R. Adler, *The Geometry of Random Fields* (Wiley, New York, 1981).  
[13] V.E. Zakharov and E.A. Kuznetsov, *Usp. Fiz. Nauk.* **167**, 1137 (1997) [*Phys. Usp.* **40**, 1087 (1997)].  
[14] M. Berning and A.M. Rubenchik, *Phys. Fluids* **10**, 1564 (1998).  
[15] S.W. Haan, *Phys. Rev. A* **39**, 5812 (1989).  
[16] J.P. Dahlburg, D.E. Fyve, G.H. Gardner, S.W. Haan, S.E. Bodner, and G.D. Doolen, *Phys. Plasmas* **2**, 2453 (1995).  
[17] M.J. Dunning and S.W. Haan, *Phys. Plasmas* **2**, 1669 (1995).  
[18] B.A. Remington, S.V. Weber, M.M. Marinak, S.W. Haan, J.D. Kilkenny, R.J. Wallace, and G. Dimonte, *Phys. Plasmas* **2**, 241 (1995).  
[19] J. Lachaise, *Thin Solid Films* **82**, 55 (1981).  
[20] S.Z. Belenkii and E.S. Fradkin, Proc. (Tr.) P.N. Lebedev Phys. Inst. **29**, 197 (1967).  
[21] K.O. Mikaelian, *Physica D* **36**, 343 (1989).  
[22] U. Alon, J. Hecht, D. Ofer, and D. Shvarts, *Phys. Rev. Lett.* **74**, 534 (1995).  
[23] C. Cherfils and K.O. Mikaelian, *Phys. Fluids* **8**, 522 (1996).  
[24] J.D. Ramshaw, *Phys. Rev. E* **58**, 5834 (1998).